

## Parton coalescence and spacetime

Dénes Molnár<sup>1</sup>

<sup>1</sup> Department of Physics, The Ohio State University,  
Columbus, OH 43210, USA

*Received September 24, 2018*

**Abstract.** The influence of spacetime dynamics in hadronization via parton coalescence at RHIC is investigated using covariant parton transport theory. Key observables, the quark number scaling of elliptic flow and the enhancement of the  $p/\pi$  ratio, show strong dynamical effects and differ from earlier results based on the simple coalescence formulas.

*Keywords:* Relativistic heavy-ion collisions, Hadronization, Quark coalescence  
*PACS:* 12.38.Mh; 24.85.+p; 25.75.Gz; 25.75.-q

### 1. Introduction

Recent exciting puzzles in  $Au + Au$  reactions at  $\sqrt{s_{NN}} = 130$  and 200 GeV at RHIC are the quark number scaling of elliptic flow [1, 2, 3] and the weaker baryon suppression than that of mesons in the intermediate transverse momentum region  $2 < p_{\perp} < 5$  GeV [1, 2, 4, 5]. Parton coalescence [6, 7, 8, 9, 10, 11, 12, 13] is probably the most promising proposal at present to explain both phenomena.

In the coalescence model, mesons form from a quark and antiquark, while baryons from three quarks or three antiquarks. The simplest version of the model is based on the “coalescence formula” (Eq. (1), or minor variation of it) that gives the hadron spectra in terms of the constituent phasespace distributions on a 3D spacetime hypersurface. Remarkably, this simple approach can reproduce quite well the particle spectra at RHIC [8, 9] and can explain the scaling of elliptic flow  $v_2(p_{\perp})$  with constituent number [10, 11]. Furthermore, the parameterizations of the constituent distributions and the hypersurface are consistent with hadronization from a thermalized quark-antiquark plasma at RHIC.

Nevertheless, these earlier studies left several important questions open. For example, it is known [10, 11] that the coalescence formula violates unitarity. The yield in a given coalescence channel scales quadratically/cubically with constituent number, moreover, the same constituent contributes to several channels (including

fragmentation in certain schemes). In addition, it is not known whether the extracted hadronization parameters (temperature, flow velocity, volume, hadronization time, etc.) are consistent with any dynamical scenario. In particular, the simple form of constituent phasespace distributions assumed ignores several kinds of phasespace correlations that would be present in a dynamical approach.

The goal of this paper is to improve upon the above deficiencies and study how the dynamics of parton coalescence affects basic observables at RHIC, such as the  $p$  and  $\pi$  suppression pattern ( $R_{AA}$ ) and elliptic flow  $v_2(p_\perp) \equiv \langle \cos \phi \rangle_{pT}$ . For simplicity, collisions at impact parameter  $b = 8$  fm ( $\approx 30\%$  centrality) are considered. Preliminary results were published in [12].

## 2. Dynamical coalescence approach

The parton coalescence formalism is largely based on studies of deuteron formation [14, 15, 16, 17]. In nonrelativistic  $N$ -body quantum mechanics, the number of deuterons (of given momentum) at time  $t$  is  $N_d(t) = N_{pairs} \text{Tr}[\hat{\rho}_d \hat{\rho}^{(2)}(t)]$ , where  $\hat{\rho}_d \equiv |\Phi_d\rangle\langle\Phi_d|$  is the deuteron density matrix,  $\hat{\rho}^{(2)}(t)$  is the projection of the density matrix  $|\Psi^{(N)}(t)\rangle\langle\Psi^{(N)}(t)|$  of the system onto the (two-particle) deuteron subspace, there are  $N_{pairs}$  possible  $n-p$  pairs, while  $\Phi_d$  and  $\Psi^{(N)}(t)$  are the wave function of the deuteron and the system. The goal is a suitable approximation for the observed deuteron number  $N_d(t \rightarrow \infty)$  because one cannot solve the full  $N$ -body problem.

One approach is to postulate that interactions *cease suddenly* at some time  $t_f$ , and approximate  $\hat{\rho}^{(2)}$  in the Wigner representation as the product of classical phase space densities  $f_n \times f_p$  on the  $t = t_f$  hypersurface. The approximation, at best, is valid for weak bound states and ignores genuine two-particle correlations. Applied to meson formation  $q\bar{q} \rightarrow M$ , one obtains the simple coalescence formula

$$\frac{dN_M(\vec{p})}{d^3p} = g_M \int \prod_{i=1,2} (d^3x_i d^3p_i) W_M(\Delta\vec{x}, \Delta\vec{p}) f_q(\vec{p}_1, \vec{x}_1) f_{\bar{q}}(\vec{p}_2, \vec{x}_2) \delta^3(\vec{p} - \vec{p}_1 - \vec{p}_2) \quad (1)$$

with  $\Delta\vec{x} \equiv \vec{x}_1 - \vec{x}_2$ ,  $\Delta\vec{p} \equiv \vec{p}_1 - \vec{p}_2$ , and the meson Wigner function  $W_M(\vec{x}, \vec{p}) \equiv \int d^3b \exp[-i\vec{b}\vec{p}] \Phi_M^*(\vec{x} - \vec{b}/2) \Phi_M(\vec{x} + \vec{b}/2)$ . The degeneracy factor  $g_M$  takes care of quantum numbers (flavor, spin, color). The formula for baryons involves a triple phasespace integral and the baryon Wigner function (which depends on two relative coordinates and two relative momenta). The generalization to arbitrary 3D hadronization hypersurfaces is straightforward [15, 17].

One difficulty with (1) is the proper choice of the hypersurface. In quantum mechanics the deuteron number is constant at *any time* after freezeout, however for free streaming (1) decreases [14, 16] with  $t_f$ . Also, transport approaches (i.e., self-consistent freezeout) yield diffuse 4D freezeout distributions [18, 19, 20], which cannot be well approximated with a hypersurface. These problems have been addressed in [14] by Gyulassy, Frankel and Remler (GFR), where they derived a way to interface transport models and the coalescence formalism in the weak binding limit.

The GFR result is the same as (1), except that the weight  $W_M$  is evaluated using the *freezeout coordinates*  $(t_1, \vec{x}_1), (t_2, \vec{x}_2)$  of each constituent pair. When taking  $\Delta\vec{x}$ , the earlier particle needs to be propagated to the time of the *later* one, resulting in an extra term, e.g.,  $\Delta\vec{x} = \vec{x}_1 - \vec{x}_2 + (t_2 - t_1)\vec{v}_1$  if  $t_1 < t_2$ . The origin of this correction is that a weak bound state can only survive if none of its constituents have any further interactions. The generalization to baryons involves propagation to the *latest* of the three freezeout times.

To investigate coalescence dynamics at RHIC, we implanted GFR into covariant parton transport theory[ 21, 22, 23, 19]. First the parton  $(g, u, d, s, \bar{u}, \bar{d}, \bar{s})$  evolution was computed until freezeout via the covariant Molnar's Parton Cascade (MPC) algorithm[ 23]. For simplicity, only  $2 \rightarrow 2$  processes were considered, with Debye-screened cross sections  $d\sigma/dt \propto 1/(t - \mu_D^2)^2$ ,  $\mu_D = 0.71$  GeV. For the total gluon-gluon cross section two values were explored,  $\sigma_{gg} = 3$  mb (the typical pQCD estimate) and 10 mb. The quark-gluon and quark-quark cross sections were suppressed by the appropriate ratio of  $SU(3)$  Casimirs:  $\sigma_{qq} = (4/9)\sigma_{gq} = (4/9)^2\sigma_{gg}$ .

At parton freezeout, the GFR formula was applied (in the two- or three-body center of mass frame) using, as common in transport approaches[ 16], box Wigner functions  $W = \prod_{i,j} \Theta(x_m - |\vec{x}_i - \vec{x}_j|)\Theta(p_m - |\vec{p}_i - \vec{p}_j|)$ , with  $x_m = 1$  fm. ( $p_m$  is fixed by the normalization for  $W$ .) This way (1) has a probabilistic interpretation: if  $W = 1$  (and the quantum numbers match) the hadron is formed, otherwise it is not ( $W = 0$ ). If several coalescence final states existed for a given constituent, one was chosen randomly with equal probability for all. Meson channels to  $\pi, K, \eta, \eta', \rho, K^*, \omega, \Phi$ ; and baryon channels to  $p, n, \Sigma, \Lambda, \Xi, \Delta, \Omega$  were considered. Gluons were assumed to split to a  $q\bar{q}$  pair with asymmetric momentum fractions  $x \approx 0$  and 1, approximated as  $1g \rightarrow 1q$  (or  $\bar{q}$ ). Easy color neutralization was also assumed. Partons that did not find a coalescence partner were fragmented independently via JETSET 7.4.10 [ 24]. JETSET was also used to decay unstable hadrons.

Because (1) requires a good sampling of full 6D phasespace, for the best statistical accuracy, quarks and antiquarks were separately flavor-averaged  $((u+d+s)/3)$  at hadronization. This assumption of flavor equilibration, which is only approximate for strange quarks, will be lifted in the future (requires longer computation).

The parton initial conditions for  $Au + Au$  at  $\sqrt{s} = 200A$  GeV at RHIC with  $b = 8$  fm were taken from [ 22]. However, as illustrated for *gluons* in Fig. 1a, for  $p_\perp > 2$  GeV LO pQCD minijet three-momentum distributions (solid line) were used (with a  $K$ -factor of 2, GRV98LO PDFs, and  $Q^2 = p_T^2$ ), which below  $p_\perp < 2$  GeV were smoothly extrapolated (circles) to yield a total parton  $dN(b=0)/dy = 2000$  at midrapidity. This choice is motivated by the observed  $dN_{ch}/dy \sim 600$  and the expectation that coalescence dominates the production. Perfect  $\eta = y$  correlation was assumed.

Figure 1a also shows that the initial condition reproduces fairly well the observed pion spectra in  $p + p$  at  $\sqrt{s} = 200$  GeV at RHIC. Binary collision scaled  $\pi_0$  data from  $p + p$  [ 25] (crosses) are compared to the isospin-averaged pion spectrum from the initial condition hadronized via either independent fragmentation in JETSET (dashed line) or BKK95 fragmentation functions [ 26] (dotted line).

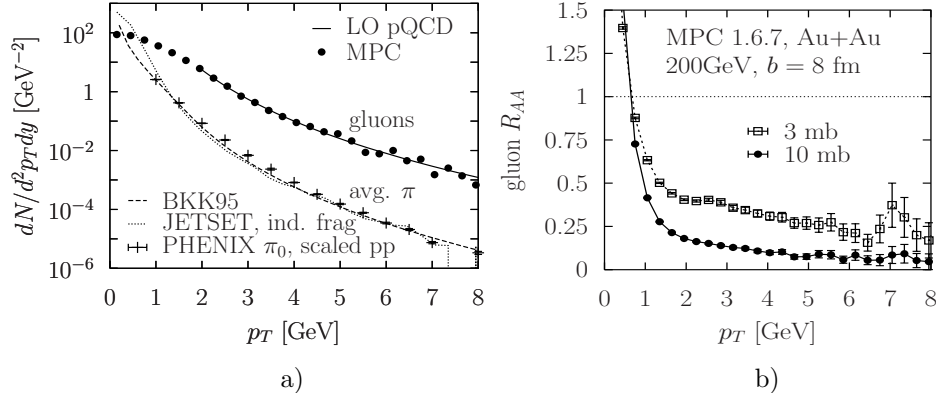


**Fig. 1.** Results for  $Au + Au$  at  $\sqrt{s} = 200A$  GeV at RHIC with  $b = 8$  fm. a) Initial gluon spectrum, and reproduction of pion spectra in  $p + p$  collisions at RHIC (see text for details); b) gluon quenching factor  $R_{AA}$  as a function of  $p_T$  for  $\sigma_{gg} = 3$  mb (open squares) and 10 mb (solid circles).

### 3. Results on spectra and elliptic flow

The final hadron momentum distributions are given by a convolution of three dynamical effects, i) the evolution of parton phasespace distributions due to multiple scatterings, ii) the hadronization process, iii) resonance decays (hadronic final state interactions were ignored).

The transport evolution *quenches* the parton spectra at high- $p_T$  by about a factor of three ( $\sigma_{gg} = 3$  mb) to ten (10 mb), as shown in Fig. 1b. The ratio  $R_{AA}$  of the parton spectrum at freezeout to the initial spectrum (which corresponds to no nuclear effects) is plotted. In the language of parton energy loss models[ 27], the suppression in this study comes from *incoherent elastic* energy loss, while in the context of hydrodynamics, it reflects the *cooling* of the expanding system due to  $pdV$  work. These results are very similar to those in Ref. [ 22] (see Fig. 9 therein), even though that study considered a pure gluon gas with *thermal* initial conditions.

Figure 2 shows the influence of coalescence dynamics on the proton and pion nuclear suppression factor  $R_{AA}$ , which is the ratio of the hadron spectra calculated from partons at freezeout to the spectra from the initial condition hadronized via *independent fragmentation* (same as binary-scaled  $p + p$ ). If only fragmentation is considered,  $R_{AA}$  for both species is about the same as that of partons (cf. Fig. 1b). On the other hand, parton coalescence enhances both pion and proton yields, and hence  $R_{AA}$ , by as much as a factor of three in the “coalescence window” [ 6, 10]  $1.5 < p_T < 4.5$  GeV. The additional hadron yield comes dominantly from partons with  $0.5 < p_T < 2$  GeV, as demonstrated in Fig. 3b, where the fraction of partons that fragment independently (i.e., that find no coalescence partner) is plotted. About two-thirds of the partons, including essentially all partons above  $p_T > 2.5$  GeV, hadronize via fragmentation.

Unfortunately, the inclusion of hadronization channels via coalescence does not

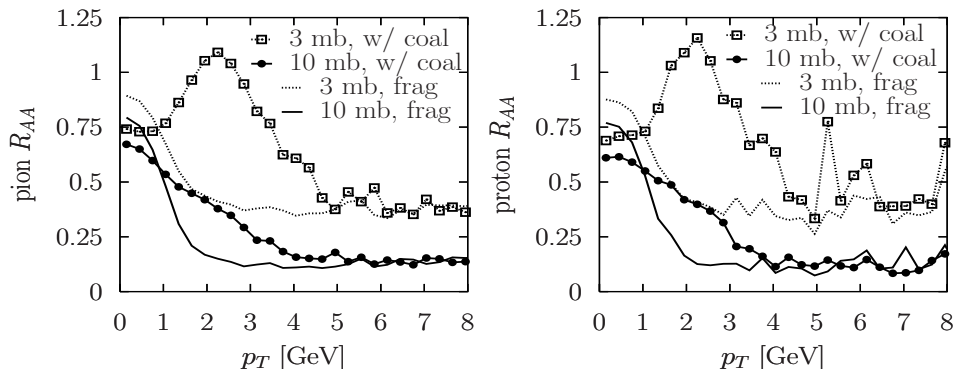


**Fig. 2.** Pion (left) and proton (right) nuclear suppression factor at RHIC in  $Au + Au$  at  $\sqrt{s} = 200A$  GeV,  $b = 8$  fm, with parton coalescence (symbols) and without coalescence (curves with no symbols), as a function of  $p_{\perp}$  and parton cross section. Results for  $\sigma_{gg} = 3$  mb (dotted) and 10 mb (solid lines) are shown.

solve the  $p/\pi$  puzzle as evident from the striking similarity between the left and right panels in Fig. 2. Though for mesons, the boundaries of the coalescence window agree well with estimates [8, 9] based on the simple coalescence formula (1), for baryons the window is about the same as for mesons and does *not* extend to higher  $p_T$ . Furthermore, the enhancement is about the same for pions and protons (protons are only  $\approx 5\%$  higher). Therefore the  $p/\pi$  ratio at intermediate  $p_T$  is the same as in  $p + p$ , while the data shows an almost two-fold increase at this centrality [4]. In fact, the pion data [28] favor  $\sigma_{gg} \approx 3$  mb ( $R_{AA}^{\pi^0} \approx 0.4$ ), while the  $p/\pi_0$  systematics [4] suggests  $R_{AA}^p \approx 1 - 1.1$ , i.e.,  $\sigma_{gg} \approx 10$  mb.

In Fig. 3a, the enhancement is characterized by  $R_{coal}$ , the ratio of the final spectra with hadronization via combined coalescence and fragmentation to that with hadronization via fragmentation only. Quite remarkably,  $R_{coal}$  is almost independent of  $\sigma_{gg}$ , despite the strong cross section dependence of the parton phase space evolution shown by the quenching (cf. Fig. 1b) and elliptic flow [22]. This very interesting aspect of parton freezeout would deserve a more detailed study.

A qualitative explanation for the above features is that compared to (1), in the weak-binding case assumed, baryon production is *disfavored* in a dynamical approach. Baryons are more fragile than mesons because they have three constituents and therefore less chance to escape without further interactions. In other words, baryons are formed at later times on average, when the densities are smaller. This meson-baryon difference, which follows from the diffuse 4D nature of self-consistent decoupling [18, 19, 20] in spacetime, is *absent* if sudden freezeout on a 3D hypersurface is postulated. To demonstrate this, we also plot in Figs. 3a-b results for a (rather unrealistic) scenario with immediate freezeout on the formation  $\tau = 0.1\text{fm}/c$  hypersurface, which does enhance the  $p/\pi$  ratio by a factor 1.5–1.7 and give a wider coalescence window for baryons.

Figure 4 shows, for  $\sigma_{gg} = 10$  mb, the effect of coalescence dynamics on pion

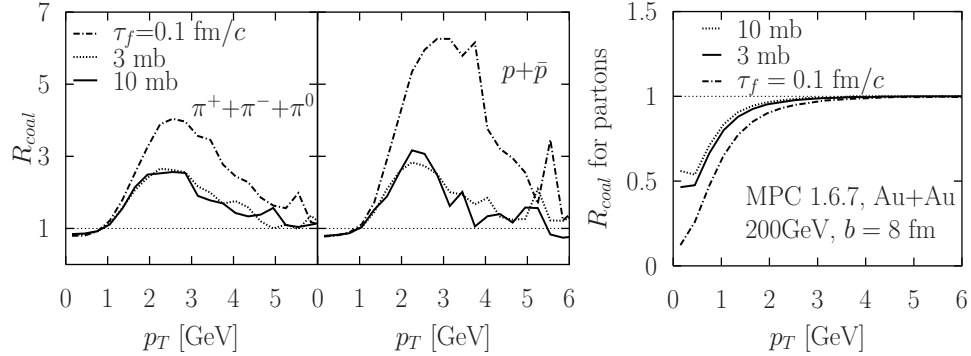


**Fig. 3.** Results for  $Au + Au$  at  $\sqrt{s} = 200A$  GeV at RHIC with  $b = 8$  fm for  $\sigma_{gg} = 3$  mb (dotted) and 10 mb (solid), or immediate freezeout at  $\tau = 0.1$  fm/c (dashed-dotted line). a) Pion and proton enhancement from parton coalescence as a function of  $p_T$ ; b) Fraction of partons that fragment independently as a function of  $p_T$ .

and proton elliptic flow, in particular on the scaling formula [6, 10]

$$v_2^{hadron}(p_T) = n v_2^{constituent}(p_T/n) \quad (2)$$

with constituent number  $n$  ( $n = 2$  for mesons, 3 for baryons). The left panel shows that the  $v_2$  of *direct* pions and protons from dynamical coalescence is smaller than predictions based on (2), by 20 and 30%, respectively. The reduction is much larger than the few-percent corrections to (2) nonlinear in  $v_2$  or those due to higher-order flow anisotropies. It is a result of dynamical coordinate-momentum correlations that were ignored in earlier approaches that assumed  $x - p$  factorizable (or even spatially uniform) constituent phasespace distributions.

The right panel in Fig. 4 shows that fragmentation contributions (and decays) further reduce the hadron  $v_2$ . Unlike the amplification from coalescence, fragmentation decreases (smears out) the anisotropy because hadrons from the parton shower are not exactly collinear with the originating parton (nonzero jet width,  $\langle |\vec{j}_\perp| \rangle > 0$ ). The parton  $v_2(p_\perp)$  extracted from the hadron flows using (2) would underpredict the real parton  $v_2$  by about a factor of two. Also, pions and protons differ on the scaling plot by at least 10%, maybe even as much as 30% (increased statistics to explore the  $p_T/n > 1 - 1.5$  GeV region is certainly desirable). A small 10 – 15% pion-proton flow scaling violation would be allowed by the published data [2, 3]. The high-statistics Run-4 data will hopefully provide much stronger constraints.

Despite the flow amplification due to coalescence, the strong reduction of  $v_2$  in the coalescence window, caused by the much smaller  $\sim 25 - 30\%$  fragmentation yield, “threatens” to reopen the opacity puzzle at RHIC [10]. The final magnitudes of proton and pion  $v_2$  are 30 – 50% below the data [3]. Large parton cross sections  $\sigma_{gg} \approx 20 - 30$  mb, an order of magnitude above pQCD estimates, would be needed to generate a large enough anisotropy, *at least in the approach presented here*.

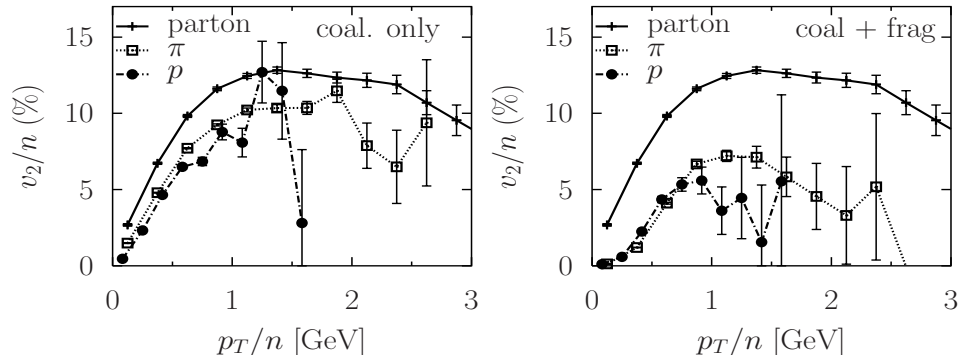


**Fig. 4.** Quark number scaled elliptic flow as a function of  $p_T$  for pions (open squares) and protons (filled circles) in  $Au+Au$  at  $\sqrt{s} = 200A$  GeV at RHIC with  $b = 8$  and  $\sigma_{gg} = 10$  mb, from hadronization via combined coalescence and fragmentation (right), and for primary hadrons (i.e., without decays) from coalescence (left). The constituent  $v_2(p_T)$  is also shown (solid lines).

#### 4. Conclusions

The above findings demonstrate that coalescence is an important hadronization channel at RHIC. However, the results also show that dynamical effects on the baryon/meson ratios and elliptic flow scaling are potentially large.

Further studies are needed to reveal what it takes to preserve the basic features of the simple coalescence formulas. It may be that the dynamics considered here was oversimplified, or the spacetime evolution in heavy-ion collisions is not understood well enough, or the QCD coalescence process cannot be approximated as a formation of weakly-bound states.

#### Acknowledgments

Computer resources by the PDSF/LBNL and the hospitality of INT Seattle where part of this work was done are gratefully acknowledged. This work was supported by DOE grant DE-FG02-01ER41190.

#### References

1. K. Schweda [STAR Collaboration], nucl-ex/0403032; M. A. C. Lamont [STAR Collaboration], nucl-ex/0403059; J. Castillo [STAR Collaboration], nucl-ex/0403027; M. Kaneta [PHENIX Collaboration], nucl-ex/0404014.
2. P. Sorensen [STAR Collaboration], *J. Phys. G* **30** (2004) S217; J. Adams *et al.* [STAR Collaboration], *Phys. Rev. Lett.* **92** (2004) 052302.
3. S. S. Adler *et al.* [PHENIX Collaboration], *Phys. Rev. Lett.* **91** (2003) 182301.

4. S. S. Adler *et al.* [PHENIX Collaboration], *Phys. Rev. Lett.* **91** (2003) 172301; *Phys. Rev. C* **69** (2004) 034909.
5. H. Long [STAR Collaboration] *J. Phys. G* **30** (2004) S193.
6. S. A. Voloshin, *Nucl. Phys. A* **715** (2003) 379.
7. R. C. Hwa and C. B. Yang, *Phys. Rev. C* **66** (2003) 025205; *ibid.* **67** (2003) 034902; hep-ph/0312271.
8. V. Greco, C. M. Ko and P. Levai, *Phys. Rev. Lett.* **90** (2003) 202302; *Phys. Rev. C* **68** (2003) 034904; V. Greco, C. M. Ko and R. Rapp, nucl-th/0312100; V. Greco and C. M. Ko, nucl-th/0402020.
9. R. J. Fries *et al.*, *Phys. Rev. Lett.* **90** (2003) 202303; *Phys. Rev. C* **68** (2003) 044902; C. Nonaka, R. J. Fries and S. A. Bass, *Phys. Lett. B* **583** (2004) 73.
10. D. Molnar and S. A. Voloshin, *Phys. Rev. Lett.* **91** (2003) 092301; D. Molnar, *J. Phys. G* **30** (2004) S235.
11. Z. w. Lin and D. Molnar, *Phys. Rev. C* **68** (2003) 044901.
12. D. Molnar, nucl-th/0403035, *J. Phys. G*, in press.
13. J. R. Fries, nucl-th/0403036; R. C. Hwa and C. B. Yang, nucl-th/0403072.
14. M. Gyulassy, K. Frankel and E. a. Remler, *Nucl. Phys. A* **402** (1983) 596.
15. C. B. Dover *et al.* *Phys. Rev. C* **44** (1991) 1636.
16. J. L. Nagle *et al.*, *Phys. Rev. C* **53** (1996) 367.
17. R. Scheibl and U. W. Heinz, *Phys. Rev. C* **59** (1999) 1585.
18. S. Soff, S. A. Bass and A. Dumitru, *Phys. Rev. Lett.* **86** (2001) 3981.
19. D. Molnar and M. Gyulassy, *Phys. Rev. C* **62** (2000) 054907; *Phys. Rev. Lett.* **92** (2004) 052301.
20. Z. w. Lin, C. M. Ko and S. Pal, *Phys. Rev. Lett.* **89** (2002) 152301.
21. B. Zhang, *Comput. Phys. Commun.* **109** (1998) 193.
22. D. Molnar and M. Gyulassy, *Nucl. Phys. A* **697** (2002) 495; *Erratum-ibid A* **703** (2002) 893.
23. D. Molnár, MPC 1.6.7. This parton transport code can be downloaded from the WWW at <http://www-cunuke.phys.columbia.edu/people/molnard> .
24. T. Sjöstrand *et al.*, *Comput. Phys. Commun.* **135** (2001) 238.
25. S. S. Adler *et al.* [PHENIX Collaboration], *Phys. Rev. Lett.* **91** (2003) 241803.
26. J. Binnewies, B. A. Kniehl and G. Kramer, *Z. Phys. C* **65** (1995) 471.
27. X. N. Wang, M. Gyulassy and M. Plumer, *Phys. Rev. D* **51** (1995) 3436; R. Baier *et al.*, *Nucl. Phys. B* **483** (1997) 291; M. Gyulassy, P. Levai and I. Vitev, *Nucl. Phys. B* **571** (2000) 197; U. A. Wiedemann, *Nucl. Phys. A* **690** (2001) 731.
28. S. S. Adler *et al.* [PHENIX Collaboration], *Phys. Rev. Lett.* **91** (2003) 072301.